Giant Epstein Tester for Magnetic Energy Loss Measurements of Non-Annealed Domain-Refined Fe–Si

Georgi Shilyashki[1], Helmut Pfützner[2], Markus Giefing[1], and Claes Bengtsson[2]

[1]Institute of Biomedical Electronics, TU Wien, 1040 Vienna, Austria
[2]ViennaMagnetics GmbH, 1020 Vienna, Austria

Since 100 years, the Epstein tester serves as a compact and simple apparatus for the measurement of magnetic energy losses, in particular for Fe–Si steel. However, drawbacks result from time-consuming cutting and stacking of the high number of just $W = 3$ cm wide sample strips of the standard Epstein tester (SET). Furthermore, the effects of cutting result in increased losses. Needs of annealing impede tests of modern materials with domain refinement that may lose its effectiveness. Results of numerical modeling indicated that both problems can be reduced by a strong enlargement of the strip width. Here, we report a novel giant Epstein tester (GET) with $W = 10$ cm, in combination with increased strip length $L = 65$ cm. Sufficient averaging over test material is attained with two layers, i.e., from just eight strips. The magnetic field strength is determined by four large 3-D-printed tangential field coils, excluding impact from the four corners of frame. Time-averaged loss P is computed from instantaneous magnetization power values p, offering also maximum loss and orientation power. Results of GET were compared to data from single-sheet tester (SST) data, proving close similarities, without needs of annealing which is significant for laser scribed steel, as tested here. Results from SET prove to be higher. Analysis of power p indicates the impact of supplementary domains in the magnetization process of the scribed material. Compared to SST, the drawbacks of the GET are the need of eight sample strips, as well as lower absolute accuracy, due to higher inhomogeneity. On the other hand, advantages are the absence of a yoke system and simplicity of test apparatus.

Index Terms— **Cutting effects, domain refinement, Epstein tester, magnetic loss, silicon iron.**

I. Introduction

SINCE decades, increased worldwide effort is aimed on a reduction of magnetic energy losses of silicon iron steel, as applied for soft magnetic cores of electric machines such as transformers, generators, and motors. Recently, the field of motors gained further relevance with the massive development of electric drives. This yields increased demand also for test systems for the measurement of the materials losses P. While the earlier focus was put on grid frequencies f of 50 and 60 Hz, modern applications stimulated increased demand also for measurements for medium frequencies, up to at least 1000 Hz.

Today, the most important tool for loss measurement has become the standardized single-sheet tester (SST) [1]. However, it suffers from very high mass, in connection with high costs. Furthermore, it includes a yoke system of massive design, in order to minimize its own power consumption. This is necessary since it is included in the measured total value of P. A neglect is possible for 50 Hz, while it may yield systematic errors for higher frequencies.

This present article is not focused on the SST but on its alternative, i.e., the so-called Epstein frame [2], in the following Epstein tester. In comparison to the SST, it offers the advantages of much lower mass and costs. Furthermore, it does not need any yoke system, thus being applicable also in the above-mentioned ranges of increased f. However, also here, the losses P are calculated from the total of power consumption. The latter includes high portions from the complex magnetization of the four corners of the quadratic frame of double-overlapped sample strips. Since decades, attempts are made to attain a separation by means of a so-called effective path length [3]–[5] or by specific substitution methods [6], [7]. However, long experience demonstrated that it is impossible to attain accurate results from these approaches.

In order to restrict the impact of corners on the total of frame, standards define very narrow sample strips, according to a width of as little as $W = 30$ mm. This reduces the mass portion of corners in advantageous ways. However, it yields an additional source of error from specific effects of sample cutting. They are initiated from the tendency that cutting of the narrow sample strips may cause severe deterioration of their magnetic characteristics in edge zones of width W_D of several millimeters [8], [9].

As it is well known, processes of "healing" are attainable by optimized annealing, but to a restricted and non-reproducible extent. Furthermore, crucial problems exist for steels that are domain refined, e.g., by laser scribing, due to the fact that the effects of treatment tend to be partly lost through annealing. Consequently, the International Electrotechnical Commission (IEC) decided that the Epstein tester should not be applied for sensitive types of material any longer [10]. Considering the high relevance of domain refined materials as the most advanced type of transformer core steel, this present article is focused on laser scribed steel.

The further-up listed advantages of Epstein tester stimulated us to construct enlarged versions of apparatus with increased strip width W, in order to decrease the impact of deteriorated edge zones as a consequence of a reduced ratio W_D/W. For a first version of a giant Epstein tester 1 (GET-1), we used a doubling of width, up to $W = 65$ mm [11]. It proved to be advantageous, however, not in complete ways.

Manuscript received December 17, 2021; revised February 2, 2022; accepted February 26, 2022. Date of publication March 14, 2022; date of current version April 25, 2022. Corresponding author: G. Shilyashki (e-mail: georgi.shilyashki@tuwien.ac.at).

Color versions of one or more figures in this article are available at https://doi.org/10.1109/TMAG.2022.3158473.

Digital Object Identifier 10.1109/TMAG.2022.3158473

This work is licensed under a Creative Commons Attribution 4.0 License. For more information, see https://creativecommons.org/licenses/by/4.0/

In this present article, we report about a further enlargement to $W = 100$ mm, which justifies the designation of a giant Epstein tester (GET) in even better ways. To predict the effectiveness of this second step, we modeled the to-be-expected modified flux distributions by means of numerical 3-D-magnetic anisotropic circuit calculation (MACC [12], [13]). These studies [14], [15] yielded encouraging results, according to the following findings.

1) The corners of an Epstein tester are magnetized with complexity that was strongly underestimated so far. For non-oriented steel, the flux goes round the inner corner edge in concentrated ways, gradually passing through the inter-laminar space. For grain-oriented steel, the flux tends to follow the rolling direction (RD). It passes into the new RD through almost homogeneous off-plane flux, taking advantage of the whole corner extent. This means that it is impossible to establish a common model for flux takeover.
2) Loss detection has to be restricted to the restricted quasi-homogeneous zone of the free limb region, which excludes to apply the standardized, so-called current method (e.g., [1], 2]).
3) Loss detection has to be based on a consistent detection of induction B and H in the quasi-homogeneous region that can be enlarged by increased strip width W.

II. Concept of GET

In its principle, the GET was constructed such as the standard Epstein tester (SET) and the first, smaller GET-version, apart from modifications that are aimed on the following.

1) To offer a sufficiently large quasi-homogeneous detection region of 100 mm width and 300 mm length, per limb. It should be useable for a physically consistent detection of field $H(t)$ and induction $B(t)$.
2) To detect $H(t)$ as close as possible to the lower surface of sample strip.
3) To allow an arrangement of sample strips in medium height of B-coil for effective compensation of air flux linked with easy insert of sample strip.

These aims were attained in satisfying ways through the following modifications.

The size of sample strips is increased from width $W = 30$ up to 100 mm and from length $L = 280$ up to 650 mm. Thus, the outer dimensions of frame are increased from 280 mm $\times$ 280 mm up to 650 mm $\times$ 650 mm, with a platform size of about 800 mm $\times$ 800 mm [Fig. 1(a)]. In obvious ways, this modification represents a compromise.

1) As a drawback, the apparatus becomes large, with needs of a power amplifier. Furthermore, a process of signal integration is needed.
2) As an advantage, the overall impact of slitting is decreased.
3) As a further advantage, the central strip regions are increased so that they can be used as rather large "detection regions," for consistent determination of B and H.

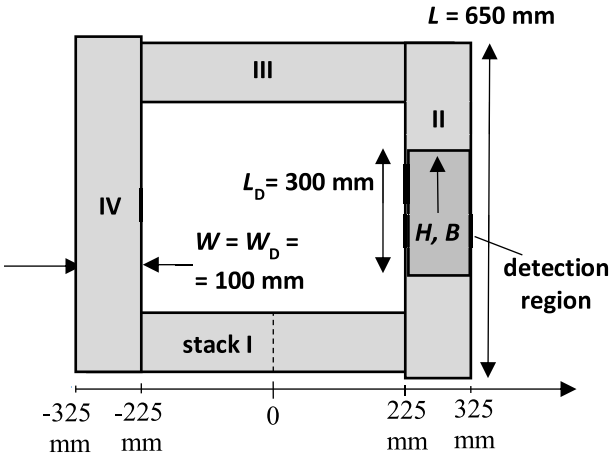

Fig. 1. Construction of GET. Schematic view from above (just one of four detection regions depicted).

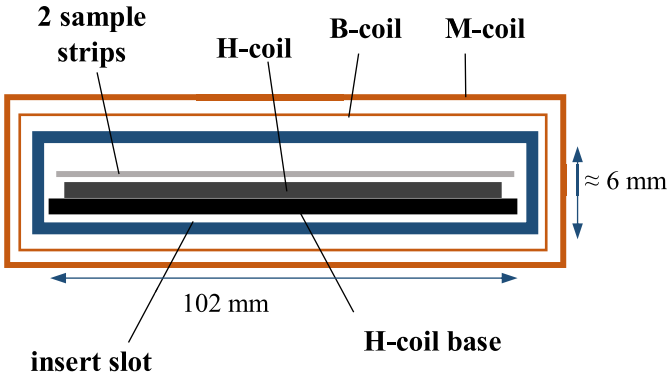

Fig. 2. Schematic outline of the cross section of one—out of four—coil units (with sample insert slot of inner 102 mm width and ca. 6 mm open height).

On the platform, four coil units were mounted, comprising elements as sketched in Fig. 2 as a cross section. The four coil formers were manufactured with a total length of 400 mm. They were created using conventional polylactic acid (PLA) filament by an extra-large 3-D printer. In order to minimize the air flux, the formers were printed without top cover. Along the inner 300 mm of each coil former, 14 even distributed grooves of 1 mm height and 5 mm width were printed (not shown in Fig. 2). The grooves assure exact positioning of the B-turns and minimizing the air flux. The sample insert slot shows a free width of 102 mm. While the open height of SET tends to be close to 20 mm, here, it is restricted to 6 mm, for a restriction of air flux. This allows for easy insert of two strips per leg.

At the bottom of each slot, a large, hybrid H-coil (compare Fig. 3) is arranged that is manufactured by 3-D printing through our so-called 3-D/2-D-assembler [16], [17] that combines the features of 3-D printing with those of 2-D printing. The overall coil dimensions are 400 mm $\times$ 100 mm $x \approx 3$ mm. In contrast to the practically unsupported H-coil of the first version of GET-1 [11], a thick 3-D-printed PLA carrier of 400 mm $\times$ 100 mm $\times$ 2 mm serves as a flat and stable substrate. It raises the active coil by 2 mm from the insert slot bottom. As a disadvantage, this increases the amount of (compensated) air flux.

Fig. 3. Photograph of one of the four tangential H-coils of 300 mm × 85 mm × 1 mm effective size, as manufactured by a semi-automatic "3-D/2-D assembler."

The active H-coil unit is printed from ca. 20 μm-thick and 300 μm-wide base winding elements of Ag, followed by ten ca. 100 μm-thick PLA layers, covered by top winding elements, and finally complemented by side elements. This yields a solid coil of low signal noise. To reduce the signal noise, the turn number per coil is just 100. However, the total active coil area results as high as 400 mm × 80 mm × 1 mm = 32 000 mm^2, a size that offers high signal intensity, for 1.7 T up to the order of 10 mV for 50 Hz and 100 mV for 400 Hz.

Placing a strip on the H-coil, its field H is detected in less than 1 mm distance from its surface. This keeps the effects of demagnetizing field to a negligible level, considering the large coil length of 300 mm. As in the case of the first version of GET, the widths of PLA layers are step-wise reduced. This reduces the effective sensitivity of edge zones that may be deteriorated through cutting. The overall field sensitivity of each coil is determined in exact ways by calibration in a circular solenoid of ca. 2000 mm length and 150 mm inner width. Due to well-defined automatic coil manufacturing, sensitivity differences prove to be weak.

For a physically consistent detection of the induction $B(t)$, a B-coil of 300 mm length is used. It evenly distributed turns of 1 mm μm-thick wire, densely arranged round the sample slot. The corresponding distance from the sample surfaces is about 4 mm, i.e., much smaller than for the SET. However, a considerably high air flux is still created. It is compensated for each sampling moment (according to a rate of 250 kHz), on the basis of the H-coil signal. While SET uses the magnetization current for air flux compensation, GET applies the actual instantaneously measured field $H(t)$. This simple solution has the additional advantage of being more accurate since $H(t)$ represents the sum field that results from the external field and the demagnetizing components of the sample strips field. As it is well known, these components show variations with increasing distance from the strip surface. However, we neglect these variations as effect of second order. Here, it should be reminded to the fact that the mutual inductor method, as used by the conventional Epstein strip tester, is based on the mere external field, under simplified assumptions.

Finally, round the B-coil, a magnetization coil is arranged with an increased length of 400 mm, in order to favor homogeneous conditions within the 300 mm-long detection region.

Loss determination is based on instantaneous values of the instantaneous magnetization power

$$p = 1/\rho \; H(t) \; dB/dt, \tag{1}$$

with ρ the density of the tested steel sample [5].

Time-averaged loss P is determined by averaging over n values p of the period T (e.g., $n = 5000$ for 50 Hz and $n = 625$ for 400 Hz) according to

$$\begin{aligned} P &= 1/(T \cdot \rho) \; {}_T\!\int H(t) \; dB/dt \\ dt &= 1/(n \cdot \rho) \; {}_{k=1,\ldots,n}\Sigma \; H_k \; (dB/dt)_k. \end{aligned} \tag{2}$$

Due to the enlarged strip width, representative results can be attained by loading with two strip layers, according to just eight strips. According to [15], this creates the problem that strips with bare end surfaces in corners show weakly decreased induction $B_1 < B$, while strips with double-embedded ends are slightly over-loaded, according to $B_2 > B > B_1$. Even higher differences result for the field strength, according to $H_2 > H > H_1$. An effective corresponding averaging is attained by averaging over the four H-coil voltages. A further reason for the evaluation of all four limbs is the fact that the latter yields improved representativeness of test results for a given steel type (of poor homogeneity). In particular, this is

valid in cases of thickness variations, e.g., due to imperfections of rolling.

For the measurements, a data acquisition card (DAQ-6361) from National Instruments (NI) with a sampling frequency of 250 kS/s is used. DAQ-6361 possesses an analog digital converter (ADC) with 16 bit resolution and with adaptive measuring range. In the used software, an adaption of the measuring range was performed, dependent on the input voltage. The magnetization of both SET and GET was performed by means of a conventional 4000 W power amplifier. The corresponding digital signal processing is performed by LabView. Exactly, sinusoidal induction, according to form factor $F = 1.111$, is attained by control of the sum voltage of M-coils for sinusoidal sum voltage of B-coils.

III. Results of Measurement

All experiments of this study were performed for a "classical" type of laser-scribed, domain refined material, as given by ZDKH [Nippon Steel Corporation (NSC)] [18] of 270 μm thickness. All tested samples were slit per guillotine from large sheets as delivered round 1985.

A. Considered Methods for Comparison of Results

A crucial problem was to decide about reference methods for an assessment of the results of measurement. As it is well known, so far, no generally accepted golden standard is existing. We considered two methods.

1) *Catalog Data as Supplied by the Manufacturer:* Data are taken from catalog [18], as determined by an SST for 600 mm length and 800 mm width. These data are restricted to losses P for 50 and 60 Hz.
2) *The Standardized SET [1]:* As well known, it derives losses P from the Watt-metrically measured power consumption of the total of magnetic circuit, comprising an indirect determination of field from the measured magnetization current. We performed tests for 50 and 60 Hz.

For the GET, eight samples of 650 mm length and 100 mm width were prepared by guillotine, carefully trying to avoid mechanical stressing and bending to a minimum. For the SET, we prepared 20 strips of 280 mm length and 30 mm width, in analogous ways.

B. Results for Time-Averaged Losses

Fig. 4 shows the results of losses P as a function of peak induction B for the technical frequencies f of 50 and 60 Hz. Results of the GET are compared with that of SET. Furthermore, results are given for an external SST.

As a clear tendency, we see that loss results P of GET are quite close to those of the SST. For high global peak induction values, even identical values are given. This can be assumed to be by incident, considering that different samples are involved, tested by completely different methods. On the other hand, the SET yielded distinctly higher results, differences exceeding the order of 10% in some cases. These deviations can be attributed to slitting effects, as reported, e.g., in [8] and [9]. Anyhow, we conclude from such results that the enlargement of Epstein

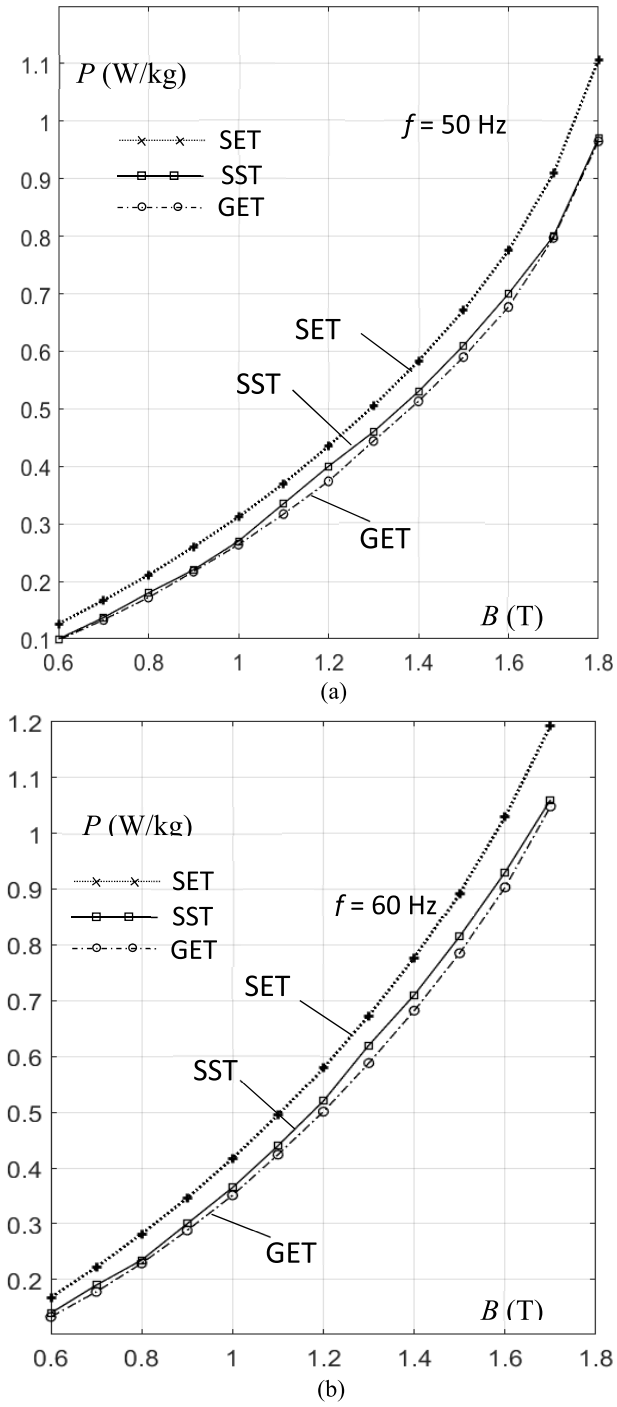

Fig. 4. Comparison of measured losses P as a function of induction peak value B, for the three investigated apparatuses. (a) 50 Hz. (b) 60 Hz.

tester—in connection with the direct determination of field—promises an increased absolute accuracy of loss measurement for technical frequencies.

Compared to SST, Epstein testers offer the general advantage to be applicable also for increased values of frequency f. Fig. 5 shows the results of measurement that have practical relevance, e.g., for e-mobility. For 100 Hz, a comparison is given between GET and SET. Similar to lower f, the GET values are lower by about 10%. For 400 Hz, the SET was not applicable. GET values prove to be above those

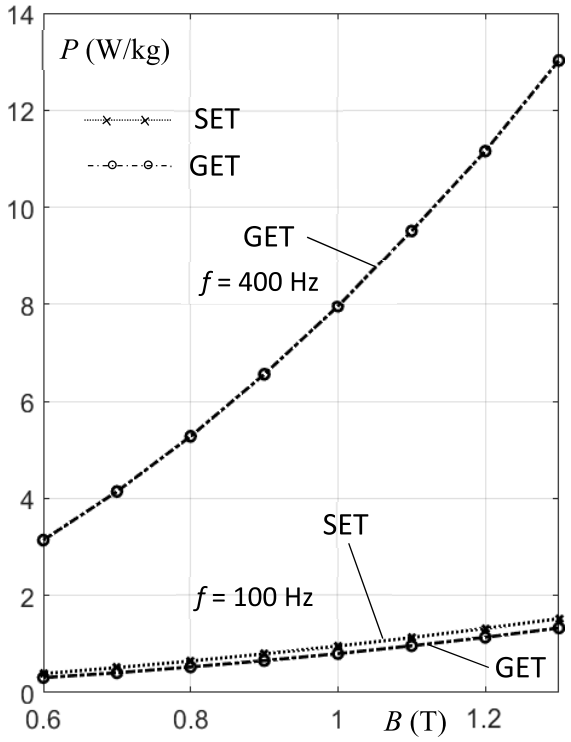

Fig. 5. Results of GET for losses P for medium-frequency values of 100 and 400 Hz. For 100 Hz, comparison values from SET are included.

for 100 Hz by factors close to 10 for the whole considered range of B.

Closer interpretations will need further study. However, the above results indicate that the GET allows for practical applications without the need of annealing, in wide ranges of both induction and frequency.

C. Results for Instantaneous Magnetization Power

According to the further above, the GET enables also the determination of magnetization power functions $p(t)$ for sinusoidal induction. The corresponding examples are given in Figs. 6 and 7.

The graphs offer significant information, as summarized in the following.

1) *Fig. 6(a) (Frequency $f = 50$ Hz With Moderate Peak Value $B = 1.5$ T of Induction):* This case yields an up-shifted 100 Hz cos function that indicates maximum instantaneous losses of $P_{\mathrm{MAX}} = 1.02$ W/kg, i.e., 73% above the averaged loss of $P = 0.59$ W/kg.
2) *Fig. 6(b) (Frequency of 50 Hz With Strong Induction of 1.8 T):* It yields a flattened 100 Hz function with $P_{\mathrm{MAX}} = 1.35$ W/kg, i.e., 40% above $P = 0.96$ W/kg. In the time interval of strong magnetization, a very weakly less pronounced second maximum is linked with a negative spike of intensity $p_{\mathrm{OR}} = 0.55$ W/kg. This orientation power value indicates spin orientation processes as needed for high instantaneous values of induction. According to 19]–[21], non-scribed highly oriented steel shows this spike in less pronounced ways. Theoretically, we interpret the orientation processes with instantaneous lancet domains, close to scribing regions as discussed in [22]. As a conclusion, the intensity of spike should be a non-linear measure for that of magnetostriction in RD, however, needing further study.
3) *Fig. 7 (Increased Frequency of 400 Hz With an Induction of 1 T):* Orientation processes are not present at 1 T, which yields a plain, up-shifted cos function of 800 Hz, without significant negative spikes.

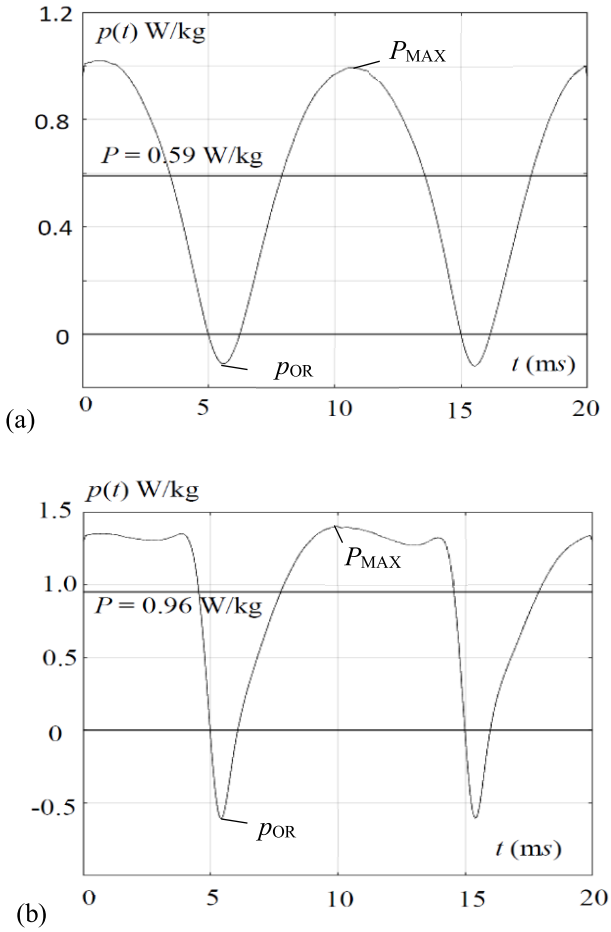

Fig. 6. Examples of instantaneous power functions $p(t)$ for $f = 50$ Hz. (a) $B = 1.5$ T. (b) $B = 1.8$ T. Notice: different ranges of scaling are used.

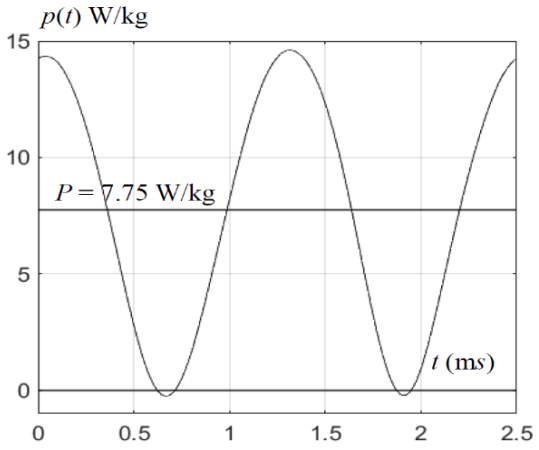

Fig. 7. Examples of instantaneous power functions $p(t)$ for $f = 400$ Hz and $B = 1$ T.

The above three cases illustrate that the determined power functions $p(t)$ can be used for multiple theoretical conclusions.

IV. Discussion and Conclusion

Considering the results of both instantaneous power p and time-averaged losses P, we conclude that the here described enlargement of Epstein tester yields a rather simply designed apparatus for loss measurements without needs for annealing. Mainly, this is proven by comparison with data from an SST that represents an apparatus of much higher complexity.

Actually, in a quite consistent way, the results of GET tend to be 10% lower than those of SET. We attribute this to two reasons.

1) Better homogeneity of the evaluated region (restricted central limb regions of GET, versus total core for the SET, including corners).
2) Much lower impact of deteriorated slitting zones.

However, we assume that Epstein testers will never be suitable for investigations that are aimed on quantitatively precise results—here, a symmetric 1-D test region can be assumed to be an undisputable request. On the other hand, an enlarged GET may be an attractive tool for comparison results, even for physically basic studies, as confirmed by measurements on instantaneous power values. However, the need of multiple sample preparation remains as an unavoidable disadvantage.

Finally, the main conclusions of the here reported study are the following.

1) The GET exhibits more than threefold width of sample strips, which reduces the effects of strip slitting in substantial ways.
2) With the increase of width and length, the number of sample strips can be reduced from about two dozens to eight strips, which reduces the expenditure of preparation work in considerable ways.
3) The indirect detection of magnetic field strength by a current measurement is replaced by the use of four "giant tangential field coils," which offers a consistent physical principle of testing.
4) Time-averaged losses are determined from a very high number of instantaneous power values that offer multiple physical information on the process of magnetization.

Acknowledgment

This work was supported by the Austrian Science Fund (FWF) through the Project "Energy Losses" under Grant P31596.

The authors would like to thank Voestalpine GmbH, Linz, Austria, and ABB Transformers, Ludvika, Sweden, for valuable contributions to the project.

References

[1] *Methods of Measurement of the Magnetic Properties of Magnetic Sheet and Strip by Means of a Single Sheet Tester*, Standard 60404-3, IEC, 1992.

[2] *Methods of Measurement of the Magnetic Properties of Magnetic Sheet and Strip by Means of an Epstein Tester*, Standard 60404-2, IEC, 1996.

[3] P. Marketos, S. Zurek, and A. J. Moses, "A method for defining the mean path length of the Epstein frame," *IEEE Trans. Magn.*, vol. 43, no. 6, pp. 2755–2757, Jun. 2007.

[4] O. de la Barriere, C. Appino, C. Ragusa, F. Fiorillo, M. LoBue, and F. Mazaleyrat, "1-D and 2-D loss-measuring methods: Optimized setup design, advanced testing, and results," *IEEE Trans. Magn.*, vol. 54, no. 9, pp. 1–15, Sep. 2018.

[5] H. Pfutzner, G. Shilyashki, and E. Huber, "Physical assessment of the magnetic path length of energy loss testers," *IEEE Trans. Magn.*, vol. 56, no. 12, pp. 1–7, Dec. 2020.

[6] G. Parent, R. Penin, J.-P. Lecointe, J.-F. Brudny, and T. Belgrand, "Determination of specific losses in the limbs of an Epstein frame using a three Epstein frame methodology applied to grain oriented electrical steels," *Sensors*, vol. 16, no. 6, p. 826, Jun. 2016.

[7] P. Marketos, S. Zurek, and A. J. Moses, "Calculation of the mean path length of the Epstein frame under non-sinusoidal excitations using the double Epstein method," *J. Magn. Magn. Mater.*, vol. 320, no. 20, pp. 2542–2545, Oct. 2008.

[8] G. Loizos and A. J. Moses, "Variation of magnetic flux density with distance from the cut edge of grain oriented electrical steel," in *Proc. Conf. ICEM*, Crete, Greece, 2006.

[9] A. Saleem, N. Alatawneh, T. Rahman, D. A. Lowther, and R. R. Chromik, "Effects of laser cutting om microstructure and magnetic properties of non-orientation electrical steel laminations," *IEEE Trans. Magn.*, vol. 56, no. 12, pp. 1–9, Oct. 2020.

[10] *IEC Revision TC 68 Meeting*, Standard 60404-8-7, 2017.

[11] G. Shilyashki, H. Pfutzner, M. Giefing, and E. Huber, "3-D printed magnetic field coil for medium frequency Epstein tester," *IEEE Trans. Magn.*, vol. 56, no. 7, pp. 1–5, Jul. 2020.

[12] G. Shilyashki, H. Pfitzner, E. Gerstbauer, G. Trenner, P. Hamberger, and M. Aigner, "Numerical prediction of rhombic rotational magnetization patterns in a transformer core package," *IEEE Trans. Magn.*, vol. 52, no. 1, pp. 1–10, Jan. 2016.

[13] H. Pfutzner, G. Shilyashki, C. Bengtsson, G. Trenner, and E. Gerstbauer, "Effects of DC bias on regional flux and magnetostriction of a single-phase transformer core modeled by 3-D MACC," *IEEE Trans. Magn.*, vol. 54, no. 5, pp. 1–6, May 2018.

[14] G. Shilyashki, H. Pfutzner, E. Huber, G. Trenner, and E. Gerstbauer, "3-D MACC modeling of instantaneous magnetic flux distributions in Epstein tester," *IEEE Trans. Magn.*, vol. 56, no. 9, pp. 1–5, Sep. 2020.

[15] G. Shilyashki, H. Pfützner, G. Trenner, C. Bengtsson, and E. Huber, "Numerical modeling of magnetic induction in standard and triple Epstein frames considering cutting and staggering of sensor strips," *AIP Adv.*, vol. 11, no. 11, Nov. 2021, Art. no. 115324.

[16] G. Shilyashki, H. Pfützner, M. Palkovits, A. Windischhofer, and M. Giefing, "3D-printed detector band for magnetic off-plane flux measurements in laminated machine cores," *Sensors*, vol. 17, no. 12, p. 2953, Dec. 2017.

[17] G. Shilyashki, H. Pfützner, Y. Kanto, U. Meisl, A. Windischhofer, and M. Giefing, "Thin band detector for analyses of rotational magnetization in laminated machine cores," *J. Magn. Magn. Mater.*, vol. 503, Jun. 2020, Art. no. 166575.

[18] *Grain-Oriented Steel Sheets*, Nippon Steel Corp., Tokyo, Japan, 1988.

[19] H. Pfützner, G. Shilyashki, C. Bengtsson, and E. Huber, "Practical aspects of instantaneous magnetization power functions of silicon iron laminations," *J. Electr. Eng. Technol.*, 2021.

[20] G. Shilyashki, H. Pfützner, C. Bengtsson, and E. Huber, "Time-averaged and instantaneous magnetic loss characteristics of different products of electrical steel for frequencies of 16 2/3 Hz up to 500 Hz," *IET Electr. Power Appl.*, vol. 2022, pp. 1–11, Jan. 2022, doi: 10.1049/elp2.12173.

[21] H. Pfützner, G. Shilyashki, and E. Huber, "Calculated vs. measured iron losses and instantaneous magnetization power functions of electrical steel," *Elect. Eng.*, pp. 1–7, Jan. 2022, doi: 10.1007/s00202-01474-4.

[22] H. Pfützner and M. Zehetbauer, "On the mechanism of domain refinement due to scratching," *Jpn. J. Appl. Phys.*, vol. 21, pp. 580–582, Sep. 1982.